



This is a repository copy of *Cobalt and chromium exposure affects osteoblast function and impairs the mineralization of prosthesis surfaces in vitro.*

White Rose Research Online URL for this paper:  
<http://eprints.whiterose.ac.uk/85661/>

Version: Accepted Version

---

**Article:**

Shah, K.M., Wilkinson, J.M. and Gartland, A. (2015) Cobalt and chromium exposure affects osteoblast function and impairs the mineralization of prosthesis surfaces in vitro. *Journal of Orthopaedic Research.*

<https://doi.org/10.1002/jor.22932>

---

**Reuse**

Unless indicated otherwise, fulltext items are protected by copyright with all rights reserved. The copyright exception in section 29 of the Copyright, Designs and Patents Act 1988 allows the making of a single copy solely for the purpose of non-commercial research or private study within the limits of fair dealing. The publisher or other rights-holder may allow further reproduction and re-use of this version - refer to the White Rose Research Online record for this item. Where records identify the publisher as the copyright holder, users can verify any specific terms of use on the publisher's website.

**Takedown**

If you consider content in White Rose Research Online to be in breach of UK law, please notify us by emailing [eprints@whiterose.ac.uk](mailto:eprints@whiterose.ac.uk) including the URL of the record and the reason for the withdrawal request.



[eprints@whiterose.ac.uk](mailto:eprints@whiterose.ac.uk)  
<https://eprints.whiterose.ac.uk/>

## Cobalt and Chromium Exposure Affects Osteoblast Function and Impairs the Mineralization of Prosthesis Surfaces *in vitro*<sup>†</sup>

Karan M. Shah<sup>a</sup>, J. Mark Wilkinson<sup>a\*</sup>, Alison Gartland<sup>a\*</sup>

<sup>a</sup>The Mellanby Centre for Bone Research, Department of Human Metabolism, The University of Sheffield, Beech Hill Road, Sheffield, S10 2RX, United Kingdom.

\*Address for correspondence: JM Wilkinson or A Gartland  
The Mellanby Centre for Bone Research  
Department of Human Metabolism  
The University of Sheffield  
Beech Hill Road  
Sheffield S10 2RX  
Fax number: +44 (0) 0114 271 2475  
Email: j.m.wilkinson@sheffield.ac.uk or a.gartland@sheffield.ac.uk

Running Title: Combined Metal Ions and Osteoblasts

### Author Contributions Statement:

Karan M. Shah – contributions to research design, acquisition, analysis and interpretation of the data and, drafting of the paper.

J. Mark Wilkinson - contributions to research design, analysis and interpretation of data, drafting of the paper and critical revisions.

A. Gartland - contributions to research design, analysis and interpretation of data, drafting of the paper and critical revisions.

All authors have read and approved the final submitted manuscript

<sup>†</sup>This article has been accepted for publication and undergone full peer review but has not been through the copyediting, typesetting, pagination and proofreading process, which may lead to differences between this version and the Version of Record. Please cite this article as doi: [10.1002/jor.22932]

Received 2 February 2015; Revised 7 April 2015; Accepted 24 April 2015

Journal of Orthopaedic Research

This article is protected by copyright. All rights reserved

DOI 10.1002/jor.22932

## ABSTRACT

Cobalt (Co) and chromium (Cr) ions and nanoparticles equivalent to those released through tribo-corrosion of prosthetic metal-on-metal (MOM) bearings and taper junctions are detrimental to osteoblast activity and function in-vitro when examined as individual species. Here we examined the effects of  $\text{Co}^{2+}:\text{Cr}^{3+}$  and  $\text{Co}^{2+}:\text{Cr}^{6+}$  combinations on osteoblast-like SaOS-2 cellular activity, alkaline phosphatase (ALP) activity and mineralization to better reflect clinical exposure conditions in vivo. We also assessed the effect of  $\text{Co}^{2+}:\text{Cr}^{3+}$  combinations and Co:Cr nanoparticles on SaOS-2 cell osteogenic responses on grit-blasted, plasma-sprayed titanium-coated and hydroxyapatite-coated prosthesis surfaces. Cellular activity and ALP activity were reduced to a greater extent with combination treatments compared to individual ions.  $\text{Co}^{2+}$  and  $\text{Cr}^{3+}$  interacted additively and synergistically to reduce cellular activity and ALP activity respectively, whilst the  $\text{Co}^{2+}$  with  $\text{Cr}^{6+}$  combination was dominated by the effect of  $\text{Cr}^{6+}$  alone. Mineralization by osteoblasts was greater on hydroxyapatite-coated surfaces compared to grit-blasted and plasma-sprayed titanium-coated surfaces. Treatments with  $\text{Co}^{2+}:\text{Cr}^{3+}$  ions and Co:Cr nanoparticles reduced the percentage mineralization on all surfaces, with hydroxyapatite-coated surfaces having the least reduction. In conclusion, our data suggests that previous studies investigating individual metal ions underestimate their potential clinical effects on osteoblast activity. Furthermore, the data suggests that hydroxyapatite-coated surfaces may modulate osteoblast responses to metal debris. This article is protected by copyright. All rights reserved

## KEYWORDS

Hip replacement; Cobalt; Chromium; Osteoblasts; Prosthesis wear; Prosthesis surfaces

## INTRODUCTION

The early failure of metal-on-metal prostheses, in part due to failures of osseointegration of cementless components, has highlighted the adverse effects of wear and corrosion mediated release of cobalt (Co) and chromium (Cr) on the periprosthetic environment<sup>1-3</sup>. Previous studies by us and others have demonstrated the detrimental effects of particulate and ionic forms of cobalt and chromium debris on osteoblast survival and function<sup>4-9</sup>. However, most studies have investigated the effects of Co and Cr ion exposure as isolated species. Whilst studying the effects of individual metal ions helps us discern their contribution to the observed detrimental effects, it does not provide us with an understanding of the effect they have in the clinical setting. Furthermore, the detrimental effects of CoCr alloy particles observed previously<sup>4; 10</sup> are likely to be mediated, at least in part, via the simultaneous exposure to Co and Cr ions as a result of their intracellular oxidation<sup>11</sup>, or dissolution in acidic lysosomal vacuoles<sup>12</sup>. Only recently, Zijlstra et al. (2011) described an increased reduction in cell number with Co<sup>2+</sup> and Cr<sup>3+</sup> combined treatment at a ratio of 1:2 compared to Co<sup>2+</sup> and Cr<sup>3+</sup> alone, to reflect clinically observed concentrations following metal-on-metal total hip arthroplasty. Study of the cellular response to combined Co and Cr ions may also highlight any additive or synergistic interactions between ions and provide mechanistic insight into downstream pathways affected.

Prosthetic surfaces are routinely modified topographically or chemically to alter their surface energy and wettability, making them more osseoconductive to promote osseointegration. Some of the most commonly used alterations to prosthesis surfaces include grit-blasting, plasma-sprayed titanium or hydroxyapatite coating. Previous studies with grit-blasted prosthesis surfaces in animal models show greater bone ongrowth observed histologically compared to polished surfaces, resulting in stronger mechanical fixation<sup>13-15</sup>. Studies have also demonstrated better bone ongrowth and fixation of hydroxyapatite-coated prosthesis

Accepted Article

surfaces compared to grit-blasted surfaces<sup>16;17</sup>. Although the effects of surface modulation on osseointegration have been extensively studied, the effect of metal ions and particles on the osteogenic response of osteoblasts on these surfaces remains unknown.

In this study we investigated the effects of clinical relevant combinations of Co and Cr ions on osteoblast activity and function. We also investigated if the interactions between the metal ions exert an additive or synergistic effect on osteoblast activity and function. Finally, we characterised the effect of prosthesis surface preparations on the osteogenic response of osteoblasts in the presence of Co/Cr ions and nanoparticles.

## METHODS

### Metal ion preparation and treatments

Cobalt (II) hexahydrate ( $\text{CoCl}_2 \cdot 6\text{H}_2\text{O}$ ) and chromium (III) chloride hexahydrate ( $\text{CrCl}_3 \cdot 6\text{H}_2\text{O}$ ) (Fluka, Gillingham, UK) served as salts for  $\text{Co}^{2+}$  and  $\text{Cr}^{3+}$  respectively. Hexavalent chromium ( $\text{Cr}^{6+}$ ) was purchased as chromium (VI) oxide ( $\text{CrO}_3$ ) from BDH Laboratory Supplies (Poole, UK). Working concentrations of each metal ion were prepared, as previously described<sup>18</sup>.

The stability of these metal ions in culture media has been confirmed previously using flame-atomic absorption spectroscopy<sup>18</sup>. Control treatment contained equivalent volume of sterile distilled water to maintain conditions, and referred to as  $0\mu\text{g/L}$  treatments.

Co and  $\text{Cr}_2\text{O}_3$  nanoparticles (a kind gift from Dr Ferdinand Lali, Imperial College, London, UK) were suspended in 100% ethanol to form a 1000X stock of the working concentration. Prior to treatments, the suspension was sonicated for 10 minutes to disaggregate the particles and diluted in osteogenic media to obtain the working concentration and observed under a microscope to confirm absence of aggregation. Control treatment contained equivalent volume of ethanol to maintain conditions.

## Activity and function assays

SaOS-2 cells were treated with a range of clinically relevant concentrations (0, 5, 50, 500 and 5000 $\mu$ g/L) of Co<sup>2+</sup>, Cr<sup>3+</sup> or a combination of Co<sup>2+</sup> and Cr<sup>3+</sup> (Co<sup>2+</sup>:Cr<sup>3+</sup>) at equal concentrations for 7 days<sup>19-24</sup>. Treatments with Cr<sup>6+</sup> ranged from (0, 5, 50 and 500 $\mu$ g/L) individually, or in combination with Co<sup>2+</sup> (Co<sup>2+</sup>:Cr<sup>6+</sup>) at equal concentrations.

## Prosthesis surfaces

Sample prosthesis surfaces were supplied by JRI Orthopaedics Ltd. (Sheffield, UK) as clinical grade titanium (Ti6Al4V) alloy sample coupons. The dimensions of each coupon were 30mmx3mm (diameter x height), for culture in 6-well plates. The surfaces were modified using the same processes as a commercial prosthesis to achieve areal surface roughness (Sz) of 57 $\mu$ m for grit-blasted, 79 $\mu$ m for plasma-sprayed titanium coated surfaces and 66 $\mu$ m for hydroxyapatite-coated surfaces respectively. The coupons were gamma-irradiated and packed in sterile conditions for subsequent cell culture.

In this study, a combination of Co<sup>2+</sup> and Cr<sup>3+</sup> at 1000 $\mu$ g/L each was used to represent the concentration of metal ions in the synovial fluid<sup>19; 25</sup>. The effect of particulate wear debris was mimicked by treating the cells with 100 nanoparticles per cell of Co and Cr oxide (mean particle diameter~30nm)<sup>26; 27</sup>.

## Osteoblast cell culture

Human osteosarcoma derived SaOS-2 osteoblast cells were cultured in T75 flasks with Dulbecco's MEM GlutaMAX™ containing 100U/mL penicillin, 100 $\mu$ g/mL streptomycin and 10% foetal bovine serum (FBS, Gibco®, Invitrogen, Paisley, UK) (referred to as complete DMEM). They were maintained at 37°C in a humidified atmosphere of 95% air and 5% CO<sub>2</sub>.

### **Cellular activity**

SaOS-2 cells were seeded in a 96-well plate at a density of  $5 \times 10^3$  cells per well in 0.2mL complete medium and left to adhere for the first 24 hours. The media was then replaced to DMEM© GlutaMAX™ containing 100U/mL penicillin, 100µg/mL streptomycin and 0.5% FBS (referred to hereon as vehicle) ± metal ion treatments till day 7 at 37°C in a humidified atmosphere of 95% air and 5% CO<sub>2</sub>. The vehicle and metal ion treatments were replenished at day 4. Cellular activity was measured at day 7 using CellTiter 96® AQueous Non-Radioactive Cell Proliferation Assay according to the manufacturer's instructions (Promega, Southampton, UK). Cellular activity was expressed as a percentage response relative to vehicle.

### **Alkaline phosphatase (ALP) activity**

SaOS-2 cells were seeded in a 96-well plate at a density of  $5 \times 10^3$  cells per well in 0.2mL complete medium and left to adhere for the first 24 hours. The media was then replaced with vehicle ± metal ion treatments till day 7 at 37°C in a humidified atmosphere of 95% air and 5% CO<sub>2</sub>. The vehicle and metal ion treatments were replenished at day 4. At day 7 the cells were washed with PBS and frozen with nuclease-free water at -80°C. ALP activity was measured by para-nitrophenyl phosphate (pNPP, Sigma-Aldrich, Dorset, UK) hydrolysis, and normalised to DNA content measured by Quant-iT™ PicoGreen® dsDNA Assay Kit (Invitrogen, Paisley, UK). The data was expressed as a percentage response relative to vehicle.

### **Mineralization Assay**

SaOS-2 cells were seeded in 48-well plates at a density of  $10 \times 10^3$  cells per well in 0.5mL complete media till they reached confluence (usually day 3). The media was then replaced

with vehicle  $\pm$  metal ion treatments supplemented with 10nM dexamethasone and 50 $\mu$ g/mL L-ascorbic acid (Sigma-Aldrich, Dorset, UK) (referred to as osteogenic media) to promote osteoblast differentiation. Vehicle  $\pm$  metal ion treatments in osteogenic media was replenished every 2-3 days until two days prior to the end of experiment, when 5mM inorganic phosphate was added to the osteogenic media to promote mineralization. On day 7 the cells were fixed overnight in 100% ethanol and stained with 40mM Alizarin Red S (pH 4.2, Sigma-Aldrich, Dorset, UK). The plates were washed extensively with 95% ethanol and air-dried prior to scanning on a flatbed scanner. The percentage area of mineralization per well was quantified using ImageJ (<http://imagej.nih.gov/ij/>) and expressed as percentage response to vehicle.

### **Mineralization on prosthesis surfaces**

Prosthesis surface mineralization was visualised by supplementing the feeding media with xylenol orange (Sigma-Aldrich, Dorset, UK), a fluorochrome that incorporates at sites of active calcification, but does not bind to hydroxyapatite coatings<sup>28-30</sup>.

Prior to cell seeding, the prosthesis surfaces were washed with PBS and pre-wetted with serum-free DMEM© GLUTAMAX™ for 60 min. SaOS-2 cells were seeded in 6-well plates containing prosthesis surfaces at a density of  $15 \times 10^4$  cells per well in 3mL complete media till they reached confluence (usually day 3). Subsequently, the cells were treated with osteogenic media containing a combination of equivalent  $\text{Co}^{2+}$  and  $\text{Cr}^{3+}$  at 1000 $\mu$ g/L, or  $15 \times 10^6$  nanoparticles each of Co and  $\text{Cr}_2\text{O}_3$ . The treatments were replenished every 2-3 days until 4 days prior to the end of experiment, when 5mM inorganic phosphate and 20 $\mu$ M xylenol orange were supplemented in the osteogenic media. On day 21, the cells were washed with PBS and fixed with 10% buffered formalin for 30min. Subsequently, the surfaces



imaged using inverted wide-field fluorescent microscope (Leica DMI 4000B) using the N3 filter. The images were analysed for percentage mineralization using ImageJ.

### **Statistical analysis**

All treatment comparisons were made to the vehicle using one-way ANOVA with Dunnett's multiple comparisons post-test or the Kruskal-Wallis test with Dunn's multiple comparisons post-test, depending on the normality of the data sets. The combinatorial effect of metal ions was analysed using the fractional-product method<sup>31</sup>. All analyses were conducted 2-tailed using a critical p-value of 0.05 using GraphPad Prism® (GraphPad Software, La Jolla, CA).

## **RESULTS**

### **Effects of Co<sup>2+</sup>, Cr<sup>3+</sup> and Cr<sup>6+</sup> combinations on SaOS-2 cellular activity**

Following 7 day exposure with individual metal ions, SaOS-2 cell activity was unaffected by all metal ions up to the concentration of 5µg/L (Figure 1A-B). Cr<sup>3+</sup> treatments decreased cellular activity at concentrations of 500µg/L (p<0.0001) and 5000µg/L (p<0.0001), which are equivalent to those observed in hip aspirates taken from patients with accelerated wear of an MOM bearing<sup>19; 25</sup> (Figure 1A). Treatments with Co<sup>2+</sup> reduced cellular activity only at the highest concentration of 5000µg/L (p<0.0001, Figure 1A). In comparison, Cr<sup>6+</sup> treatments reduced cell activity at concentrations of 50µg/L (p<0.0001), and 500µg/L (p<0.0001, Figure 1B).

When SaOS-2 cells were treated with the Co<sup>2+</sup>:Cr<sup>3+</sup> combination at 5000µg/L, an additive effect was observed, with a lower cell activity compared to treatment with Co<sup>2+</sup> or Cr<sup>3+</sup> in isolation (p<0.0001, Figure 1A). No further decrease in cell activity was observed for Co<sup>2+</sup>:Cr<sup>6+</sup> combination treatment compared to Cr<sup>6+</sup> alone (Figure 1B).

### **Effects of Co<sup>2+</sup>, Cr<sup>3+</sup> and Cr<sup>6+</sup> combinations on SaOS-2 ALP activity**

The ALP activity of SaOS-2 cells remained unaffected following 7 day treatment with individual metal ions up to the concentration of 50µg/L (Figure 2A-B). Co<sup>2+</sup> and Cr<sup>3+</sup> treatments caused a reduction in ALP activity at 5000µg/L (p<0.0001, Figure 2A). Cr<sup>6+</sup> treatment reduced ALP activity at a lower concentration of 500µg/L (p<0.0001, Figure 2B). When SaOS-2 cells were treated with a combination of Co<sup>2+</sup>:Cr<sup>3+</sup>, a synergistic interaction was observed that further reduced the ALP activity compared to individual Co<sup>2+</sup> and Cr<sup>3+</sup> treatments at 5000µg/L (p<0.0001, Figure 2A). Co<sup>2+</sup>:Cr<sup>6+</sup> combined treatment had a biphasic effect with an increase in ALP activity at 5µg/L (p<0.01) and a decrease at higher concentrations of 50µg/L (p<0.0001) and 500 µg/L (p<0.0001) compared to vehicle (Figure 2B). The ALP activity with Co<sup>2+</sup>:Cr<sup>6+</sup> combined treatment was lower compared to 50µg/L Co<sup>2+</sup> (p<0.05) and, 500µg/L of Co<sup>2+</sup> (p<0.0001) or Cr<sup>6+</sup> (p<0.05, Figure 2B).

### **Effects of Co<sup>2+</sup>, Cr<sup>3+</sup> and Cr<sup>6+</sup> combinations on SaOS-2 mineralization**

The percentage mineralization of SaOS-2 cells when grown in osteogenic media was reduced at concentrations of metal ions equivalent to those found in hip synovial fluid in patients with accelerated MOM bearing wear. Co<sup>2+</sup> treatment at 5000µg/L reduced the percentage mineralization compared to vehicle (p<0.0001), whilst a reduction in mineralization was observed with Cr<sup>3+</sup> treatments at 500µg/L (p<0.01) and 5000µg/L (p<0.0001, Figure 3A). Cr<sup>6+</sup> treatments elicited a biphasic response with an increase in percentage mineralization at concentration equivalent to serum concentrations (p<0.01 at 5µg/L) and a decrease in mineralization at concentrations equivalent to hip synovial fluid concentrations (p<0.0001 at 500µg/L, Figure 3B).

Combined Co<sup>2+</sup>:Cr<sup>3+</sup> exposure also induced a biphasic response, with an increase in the percentage mineralization at 500µg/L (p<0.05) and a decrease at 5000µg/L (p<0.0001)

Accepted Article

compared to the vehicle (Figure 3A). The increase in percentage mineralization with 500 $\mu$ g/L of Co<sup>2+</sup>:Cr<sup>3+</sup> was also higher compared to Co<sup>2+</sup> and Cr<sup>3+</sup> individually (p<0.0001, Figure 3A). A reduction in percentage mineralization was observed with 500 $\mu$ g/L (p<0.0001) Co<sup>2+</sup>:Cr<sup>6+</sup> combined treatment, similar to the effect of Cr<sup>6+</sup> alone (Figure 3B). The Co<sup>2+</sup> and Cr<sup>6+</sup> combinations did not exhibit any interactions.

### **Effect of metal ions and nanoparticles on ALP activity of SaOS-2 cells grown on prosthesis surfaces**

When SaOS-2 cells were grown on hydroxyapatite-coated surfaces without metal exposure, the ALP activity was lower compared to that observed on grit-blasted or plasma-sprayed titanium surfaces (p<0.0001, Figure 4).

In the presence of the Co<sup>2+</sup>:Cr<sup>3+</sup> metal ion combination, the ALP activity of SaOS-2 cells grown on hydroxyapatite-coated surfaces remain unchanged compared to vehicle, whilst a reduction was observed for cells grown on grit-blasted (p<0.05) and plasma-sprayed titanium surfaces (p<0.0001, Figure 4). Treatments with Co:Cr nanoparticles also reduced the ALP activity for plasma-sprayed titanium surfaces (p<0.0001), whilst it remained unchanged for cells grown on hydroxyapatite-coated and grit-blasted surfaces (Figure 4).

The ALP activity for cells cultured on hydroxyapatite coated surfaces remained lower compared to the grit-blasted or plasma-sprayed titanium surfaces in the presence of Co<sup>2+</sup>:Cr<sup>3+</sup> (p<0.01) and Co:Cr nanoparticles (p<0.01 and p<0.05 respectively, Figure 4). There was no difference in ALP activity observed for cells grown on grit-blasted and plasma-sprayed titanium surfaces for all conditions.

### **Effect of metal ions and nanoparticles on mineralization activity of SaOS-2 cells grown on prosthesis surfaces**

When SaOS-2 cells were grown on hydroxyapatite-coated surfaces, the percentage mineralization was greater compared to cells grown on grit-blasted or titanium plasma-sprayed surfaces ( $P < 0.0001$ , Figure 5B). The percentage mineralization on grit-blasted surfaces was also higher compared to mineralization on titanium plasma-sprayed surfaces ( $p < 0.05$ , Figure 5B).

When SaOS-2 cells were grown on hydroxyapatite-coated surfaces in the presence of  $\text{Co}^{2+}:\text{Cr}^{3+}$  metal ions or Co:Cr nanoparticles, the percentage mineralization was reduced by 21% and 36%, respectively, compared to vehicle ( $p < 0.0001$ , Figure 6). For grit-blasted surfaces, a 48% reduction in percentage mineralization was observed with  $\text{Co}^{2+}:\text{Cr}^{3+}$  metal ion treatments, whilst treatment with Co-Cr nanoparticles reduced percentage mineralization by 99% ( $p < 0.0001$ ). When the cells were grown on plasma-sprayed titanium surfaces, a reduction of 86% and 88% in percentage mineralization was observed with  $\text{Co}^{2+}:\text{Cr}^{3+}$  metal ions or Co:Cr nanoparticles treatments, respectively, compared to vehicle ( $p < 0.0001$ , Figure 6). The decrease in percentage mineralization in the presence of  $\text{Co}^{2+}:\text{Cr}^{3+}$  metal ions or Co:Cr nanoparticles was less for hydroxyapatite-coated surfaces compared to grit-blasted or plasma-sprayed titanium surfaces ( $P < 0.0001$ , Figure 6).

## DISCUSSION

In this study we examined the effects of  $\text{Co}^{2+}$ ,  $\text{Cr}^{3+}$  and  $\text{Cr}^{6+}$  on human osteoblast-like cell activity, ALP activity and mineralization in vitro, at clinically relevant concentrations and those found in patients after MOM hip resurfacing or hip replacement<sup>19-24</sup>. A greater detrimental effect on cell activity and function was observed with metal ion combinations compared to individual metal ions. Co and Cr ions or nanoparticles also reduced the osteogenic response of osteoblasts grown on prosthetic surfaces, and this effect varied with surface preparations.

Our findings are consistent with the previously described detrimental effects with individual ions on osteoblast cellular activity *in vitro*<sup>6; 7</sup>. In addition, we demonstrate an additive detrimental effect on cell activity with chronic exposure to  $\text{Co}^{2+}:\text{Cr}^{3+}$  at concentrations reported in the synovial fluid of some patients with a MOM bearing<sup>19; 25</sup>. The observed additive effect implies the existence of common downstream mechanisms for the effect of both  $\text{Co}^{2+}$  and  $\text{Cr}^{3+}$  on osteoblast function. Amongst other mechanisms of action, the participation of  $\text{Co}^{2+}$  and  $\text{Cr}^{3+}$  in Fenton-like reactions resulting in oxidative DNA damage<sup>32; 33</sup>, and disruption of DNA replication and repair<sup>34-36</sup>, may cause the observed additive effects. This is consistent with a study that describes a similar additive effect for iron ( $\text{Fe}^{2+}$ ) and  $\text{Cr}^{3+}$  combination on Fenton-like reaction mediated oxidative DNA damage<sup>37</sup>. The similarity in the chemical characteristics of  $\text{Fe}^{2+}$  and  $\text{Co}^{2+}$  might result in similar additive effects with  $\text{Co}^{2+}$  and  $\text{Cr}^{3+}$ .

In contrast to  $\text{Co}^{2+}:\text{Cr}^{3+}$ , the combined effect of  $\text{Co}^{2+}:\text{Cr}^{6+}$  at high concentrations is dominated by  $\text{Cr}^{6+}$  toxicity with no additive or synergistic effects.  $\text{Cr}^{6+}$  is a known carcinogen and its high toxicity has been studied extensively for different cell types including osteoblasts<sup>6; 38</sup>. This high toxicity is likely to mask any interactions with  $\text{Co}^{2+}$ .

The osteogenic response of osteoblasts, assessed by ALP activity and mineralization, was reduced with individual  $\text{Co}^{2+}$ ,  $\text{Cr}^{3+}$  or  $\text{Cr}^{6+}$  treatment at concentrations equivalent to that found in the synovial fluid from some patients with MOM bearings, consistent with previous study findings<sup>6; 39</sup>. Simultaneous  $\text{Co}^{2+}$  and  $\text{Cr}^{3+}$  treatment resulted in synergistic interactions to reduce ALP activity, suggesting separate downstream actions. Alkaline phosphatase is a highly conserved metalloenzyme containing two  $\text{Zn}^{2+}$  centres which are vital to its catalytic activity<sup>40; 41</sup>. Previous studies have described substitution of  $\text{Zn}^{2+}$  by  $\text{Co}^{2+}$  in a variety of proteins including ALP, resulting in reduced ALP enzymatic activity<sup>42</sup>. In contrast, the effects with  $\text{Cr}^{3+}$  may be more indirect with induced cellular stress resulting in a reduction in

ALP production<sup>43</sup>. The increase in mineralization observed with 500µg/L Co<sup>2+</sup>:Cr<sup>3+</sup> treatment compared to individual metal ions is an unexpected finding. Whilst the exact mechanism for this remains unclear, there is evidence which suggests that apoptotic or necrotic cell bodies are associated with nucleation of the collagen matrix around which mineralization could progress<sup>44-47</sup>. The previous report by Zijlstra et al. (2011) also described a greater reduction in cell number with combined treatments compared to individual metal ions, which might result in a slight increase in the nucleation of the matrix and subsequent mineralization.

Whilst these studies suggest a detrimental effect of metal ions on prosthesis osseointegration and speculate on the possible mechanisms involved, they do not inform us about the role that prosthesis surface preparations may play in the osteogenic response of osteoblasts at the prosthesis-bone interface. This was assessed by measuring osteoblast ALP activity and mineralization on routinely used prosthesis surface preparations with and without exposure to Co<sup>2+</sup>:Cr<sup>3+</sup> metal ion combination or Co:Cr nanoparticles. Our study shows that the whilst the ALP activity of osteoblasts grown on hydroxyapatite-coated surfaces is lower compared to cells grown on grit-blasted and plasma-sprayed titanium-coated surfaces, their ability to mineralise is much higher. This is suggestive of accelerated cellular differentiation on hydroxyapatite-coated surfaces, with an early peaking of ALP activity and its reduction prior to the increase in mineralization<sup>48-50</sup>. This is supported by the greater osteoconductivity of hydroxyapatite-coated surfaces reported previously<sup>51; 52</sup>. In presence of metal ions or nanoparticles, the ALP activity remained unchanged for cells on hydroxyapatite-coated surfaces, whereas a reduction was observed for both grit-blasted and plasma-sprayed titanium-coated surfaces compared to untreated controls. Moreover, whilst the mineralization on hydroxyapatite-coated surfaces was reduced with metal ions or nanoparticles, the reduction for both grit-blasted and plasma-sprayed titanium-coated surfaces was more severe. Thus, hydroxyapatite-coated surfaces may help protect the osteogenic activity of metal-

exposed osteoblasts. These results are consistent with clinical data from the National Joint Registry of England and Wales, which show a 5-year revision rate of 3.9% (95%CI, 3.6-4.2) for the Birmingham and 5% (4.2-5.9) for Adept hip resurfacing systems that use a hydroxyapatite-coated acetabular prostheses, compared to 8.1% (6.7-9.8) for the Conserve Plus and 5.9% (4.8-7.2) for the Durom resurfacing that use a plasma-sprayed titanium coating<sup>1</sup>.

This study has several limitations. The use of primary human cells to determine the effects of metal ions or nanoparticles would be more relevant to the clinical situation. However, a recent study has demonstrated similar gene expression profiles, ALP activity and mineralization profiles between SaOS-2 cells and primary human osteoblasts<sup>48</sup>. The use of Co and Cr ion combinations at the ratio of 1:1 is a representative approximation of the in vivo environment after hip resurfacing (but may differ in MOM hip replacement), but may vary clinically between patients. Finally, although commercially sourced Co and Cr nanoparticles are commonly used to describe tissue effects associated with MOM bearings<sup>53</sup>, the use of alloy wear particles generated clinically would be of more direct physiological relevance. In conclusion, our findings highlight species and concentration dependent interactions between Co and Cr ions, and show that assessment of their effects when used in combination is likely to be of more clinical relevance than evaluation of the isolated effects of individual ions. Finally, our data suggest that prosthesis surface coating may be a factor that modulates the effect of metal exposure on prosthesis osseointegration and survival.

## ACKNOWLEDGEMENTS

The authors would like to thank Dr Ferdinand Lali (Imperial College, London, UK) for providing the nanoparticles, and JRI Orthopaedics Ltd. (Sheffield, UK) for providing the prosthesis surface preparations used in this study. This research was funded by a National Institute for Health Research Biomedical Research Fellowship (BRF-2011-013 and BRF-2011-020).



**REFERENCES**

1. NJR. 2014. National Joint Registry 11th Annual Report. National Joint registry of England and Wales.
2. Smith AJ, Dieppe P, Howard PW, et al. 2012. Failure rates of metal-on-metal hip resurfacings: analysis of data from the National Joint Registry for England and Wales. *Lancet* 380:1759-1766.
3. Smith AJ, Dieppe P, Vernon K, et al. 2012. Failure rates of stemmed metal-on-metal hip replacements: analysis of data from the National Joint Registry of England and Wales. *Lancet* 379:1199-1204.
4. Dalal A, Pawar V, McAllister K, et al. 2012. Orthopedic implant cobalt-alloy particles produce greater toxicity and inflammatory cytokines than titanium alloy and zirconium alloy-based particles in vitro, in human osteoblasts, fibroblasts, and macrophages. *J Biomed Mater Res A* 100:2147-2158.
5. Lochner K, Fritsche A, Jonitz A, et al. 2011. The potential role of human osteoblasts for periprosthetic osteolysis following exposure to wear particles. *Int J Mol Med* 28:1055-1063.
6. Andrews RE, Shah KM, Wilkinson JM, et al. 2011. Effects of cobalt and chromium ions at clinically equivalent concentrations after metal-on-metal hip replacement on human osteoblasts and osteoclasts: implications for skeletal health. *Bone* 49:717-723.
7. Fleury C, Petit A, Mwale F, et al. 2006. Effect of cobalt and chromium ions on human MG-63 osteoblasts in vitro: morphology, cytotoxicity, and oxidative stress. *Biomaterials* 27:3351-3360.
8. Anissian L, Stark A, Dahlstrand H, et al. 2002. Cobalt ions influence proliferation and function of human osteoblast-like cells. *Acta Orthop Scand* 73:369-374.

9. Zijlstra WP, Bulstra SK, van Raay JJ, et al. 2012. Cobalt and chromium ions reduce human osteoblast-like cell activity in vitro, reduce the OPG to RANKL ratio, and induce oxidative stress. *J Orthop Res* 30:740-747.
10. Allen MJ, Myer BJ, Millett PJ, et al. 1997. The effects of particulate cobalt, chromium and cobalt-chromium alloy on human osteoblast-like cells in vitro. *J Bone Joint Surg Br* 79:475-482.
11. Shahgaldi BF, Heatley FW, Dewar A, et al. 1995. In vivo corrosion of cobalt-chromium and titanium wear particles. *J Bone Joint Surg Br* 77:962-966.
12. Lohmann CH, Schwartz Z, Koster G, et al. 2000. Phagocytosis of wear debris by osteoblasts affects differentiation and local factor production in a manner dependent on particle composition. *Biomaterials* 21:551-561.
13. Abe L, Nishimura I, Izumisawa Y. 2008. Mechanical and histological evaluation of improved grit-blast implant in dogs: pilot study. *J Vet Med Sci* 70:1191-1198.
14. Feighan JE, Goldberg VM, Davy D, et al. 1995. The influence of surface-blasting on the incorporation of titanium-alloy implants in a rabbit intramedullary model. *J Bone Joint Surg Am* 77:1380-1395.
15. Jinno T, Goldberg VM, Davy D, et al. 1998. Osseointegration of surface-blasted implants made of titanium alloy and cobalt-chromium alloy in a rabbit intramedullary model. *J Biomed Mater Res* 42:20-29.
16. Eckardt A, Aberman HM, Cantwell HD, et al. 2003. Biological fixation of hydroxyapatite-coated versus grit-blasted titanium hip stems: a canine study. *Arch Orthop Trauma Surg* 123:28-35.
17. Park YS, Yi KY, Lee IS, et al. 2005. The effects of ion beam-assisted deposition of hydroxyapatite on the grit-blasted surface of endosseous implants in rabbit tibiae. *Int J Oral Maxillofac Implants* 20:31-38.

18. Andrews RE, Shah KM, Wilkinson JM, et al. 2011. Effects of cobalt and chromium ions at clinically equivalent concentrations after metal-on-metal hip replacement on human osteoblasts and osteoclasts: Implications for skeletal health. *Bone*.
19. Davda K, Lali FV, Sampson B, et al. 2011. An analysis of metal ion levels in the joint fluid of symptomatic patients with metal-on-metal hip replacements. *The Journal of bone and joint surgery British volume* 93:738-745.
20. De Pasquale D, Stea S, Squarzone S, et al. 2014. Metal-on-metal hip prostheses: correlation between debris in the synovial fluid and levels of cobalt and chromium ions in the bloodstream. *Int Orthop* 38:469-475.
21. Langton DJ, Jameson SS, Joyce TJ, et al. 2010. Early failure of metal-on-metal bearings in hip resurfacing and large-diameter total hip replacement: A consequence of excess wear. *J Bone Joint Surg Br* 92:38-46.
22. Langton DJ, Sprowson AP, Joyce TJ, et al. 2009. Blood metal ion concentrations after hip resurfacing arthroplasty: a comparative study of articular surface replacement and Birmingham Hip Resurfacing arthroplasties. *J Bone Joint Surg Br* 91:1287-1295.
23. Moroni A, Savarino L, Cadossi M, et al. 2008. Does ion release differ between hip resurfacing and metal-on-metal THA? *Clin Orthop Relat Res* 466:700-707.
24. Williams DH, Greidanus NV, Masri BA, et al. 2011. Prevalence of pseudotumor in asymptomatic patients after metal-on-metal hip arthroplasty. *J Bone Joint Surg Am* 93:2164-2171.
25. Kwon YM, Ostlere SJ, McLardy-Smith P, et al. 2011. "Asymptomatic" pseudotumors after metal-on-metal hip resurfacing arthroplasty: prevalence and metal ion study. *J Arthroplasty* 26:511-518.
26. Polyzois I, Nikolopoulos D, Michos I, et al. 2012. Local and systemic toxicity of nanoscale debris particles in total hip arthroplasty. *J Appl Toxicol* 32:255-269.

27. Brown C, Williams S, Tipper JL, et al. 2007. Characterisation of wear particles produced by metal on metal and ceramic on metal hip prostheses under standard and microseparation simulation. *J Mater Sci Mater Med* 18:819-827.
28. Shu R, McMullen R, Baumann MJ, et al. 2003. Hydroxyapatite accelerates differentiation and suppresses growth of MC3T3-E1 osteoblasts. *J Biomed Mater Res A* 67:1196-1204.
29. Wang YH, Liu Y, Maye P, et al. 2006. Examination of mineralized nodule formation in living osteoblastic cultures using fluorescent dyes. *Biotechnol Prog* 22:1697-1701.
30. Kuhn LT, Liu Y, Advincula M, et al. 2010. A nondestructive method for evaluating in vitro osteoblast differentiation on biomaterials using osteoblast-specific fluorescence. *Tissue Eng Part C Methods* 16:1357-1366.
31. Chou TC, Talalay P. 1984. Quantitative analysis of dose-effect relationships: the combined effects of multiple drugs or enzyme inhibitors. *Adv Enzyme Regul* 22:27-55.
32. Leonard S, Gannett PM, Rojanasakul Y, et al. 1998. Cobalt-mediated generation of reactive oxygen species and its possible mechanism. *J Inorg Biochem* 70:239-244.
33. Tsou TC, Yang JL. 1996. Formation of reactive oxygen species and DNA strand breakage during interaction of chromium (III) and hydrogen peroxide in vitro: evidence for a chromium (III)-mediated Fenton-like reaction. *Chemico-biological interactions* 102:133-153.
34. Dai H, Liu J, Malkas LH, et al. 2009. Chromium reduces the in vitro activity and fidelity of DNA replication mediated by the human cell DNA synthesome. *Toxicol Appl Pharmacol* 236:154-165.

35. El-Yamani N, Zuniga L, Stoyanova E, et al. 2011. Chromium-induced genotoxicity and interference in human lymphoblastoid cell (TK6) repair processes. *J Toxicol Environ Health A* 74:1030-1039.
36. Kopera E, Schwerdtle T, Hartwig A, et al. 2004. Co(II) and Cd(II) substitute for Zn(II) in the zinc finger derived from the DNA repair protein XPA, demonstrating a variety of potential mechanisms of toxicity. *Chem Res Toxicol* 17:1452-1458.
37. Moriwaki H, Osborne MR, Phillips DH. 2008. Effects of mixing metal ions on oxidative DNA damage mediated by a Fenton-type reduction. *Toxicol In Vitro* 22:36-44.
38. Ning J, Grant MH. 1999. Chromium (VI)-induced cytotoxicity to osteoblast-derived cells. *Toxicol In Vitro* 13:879-887.
39. Dai M, Zhou T, Xiong H, et al. 2011. [Effect of metal ions  $\text{Co}^{2+}$  and  $\text{Cr}^{3+}$  on osteoblast apoptosis, cell cycle distribution, and secretion of alkaline phosphatase]. *Zhongguo Xiu Fu Chong Jian Wai Ke Za Zhi* 25:56-60.
40. Stec B, Holtz KM, Kantrowitz ER. 2000. A revised mechanism for the alkaline phosphatase reaction involving three metal ions. *J Mol Biol* 299:1303-1311.
41. Kozlenkov A, Manes T, Hoylaerts MF, et al. 2002. Function assignment to conserved residues in mammalian alkaline phosphatases. *J Biol Chem* 277:22992-22999.
42. Wang J, Stieglitz KA, Kantrowitz ER. 2005. Metal specificity is correlated with two crucial active site residues in *Escherichia coli* alkaline phosphatase. *Biochemistry* 44:8378-8386.
43. Rudolf E, Cervinka M. 2009. Trivalent chromium activates Rac-1 and Src and induces switch in the cell death mode in human dermal fibroblasts. *Toxicol Lett* 188:236-242.

44. Lynch MP, Capparelli C, Stein JL, et al. 1998. Apoptosis during bone-like tissue development in vitro. *J Cell Biochem* 68:31-49.
45. Zimmermann B. 1992. Degeneration of osteoblasts involved in intramembranous ossification of fetal rat calvaria. *Cell and tissue research* 267:75-84.
46. Hashimoto S, Ochs RL, Rosen F, et al. 1998. Chondrocyte-derived apoptotic bodies and calcification of articular cartilage. *Proc Natl Acad Sci U S A* 95:3094-3099.
47. Zimmermann B. 1994. Occurrence of osteoblast necroses during ossification of long bone cortices in mouse fetuses. *Cell and tissue research* 275:345-353.
48. Czekanska EM, Stoddart MJ, Ralphs JR, et al. 2013. A phenotypic comparison of osteoblast cell lines versus human primary osteoblasts for biomaterials testing. *J Biomed Mater Res A*.
49. Genge BR, Sauer GR, Wu LN, et al. 1988. Correlation between loss of alkaline phosphatase activity and accumulation of calcium during matrix vesicle-mediated mineralization. *J Biol Chem* 263:18513-18519.
50. Stein GS, Lian JB, Owen TA. 1990. Relationship of cell growth to the regulation of tissue-specific gene expression during osteoblast differentiation. *FASEB journal* : official publication of the Federation of American Societies for Experimental Biology 4:3111-3123.
51. Malik MA, Puleo DA, Bizios R, et al. 1992. Osteoblasts on hydroxyapatite, alumina and bone surfaces in vitro: morphology during the first 2 h of attachment. *Biomaterials* 13:123-128.
52. Okumura A, Goto M, Goto T, et al. 2001. Substrate affects the initial attachment and subsequent behavior of human osteoblastic cells (Saos-2). *Biomaterials* 22:2263-2271.

53. Kwon YM, Xia Z, Glyn-Jones S, et al. 2009. Dose-dependent cytotoxicity of clinically relevant cobalt nanoparticles and ions on macrophages in vitro. *Biomed Mater* 4:025018.

**Figure 1. Effect of metal ion combinations on osteoblast activity**

Cellular activity of SaOS-2 cells was measured using an MTS assay, after 7 day treatments with metal ions. The graphs are depicted with metal ion concentrations compartmentalised corresponding to physiological, patient serum and patient hip aspirate levels post metal-on-metal hip replacements (MOMHR). **A)** The effect of  $\text{Co}^{2+}:\text{Cr}^{3+}$  combinations at equal concentrations, and **B)** the effect of  $\text{Co}^{2+}:\text{Cr}^{6+}$  combinations at equal concentrations. All values (mean  $\pm$  95%CI) are expressed relative to the vehicle (100%). n = 4-6 wells per experiment, 3 replicate experiments. \* <sup>a</sup> p<0.05, \*\* <sup>b</sup> p<0.01 and \*\*\* <sup>c</sup> p<0.0001.

**Figure 2. Effect of metal ion combinations on osteoblast ALP activity**

ALP activity of SaOS-2 cells normalised to dsDNA after 7 day treatments with metal ions. The graphs are depicted with metal ion concentrations compartmentalised corresponding to physiological, patient serum and patient hip aspirate levels post MOMHR. **A)** The effect of  $\text{Co}^{2+}:\text{Cr}^{3+}$  combinations at equal concentrations, and **B)** the effect of  $\text{Co}^{2+}:\text{Cr}^{6+}$  combinations at equal concentrations. All values (mean  $\pm$  95%CI) are expressed relative to the vehicle (100%). n = 4-6 wells per experiment, 3 replicate experiments. \* <sup>a</sup> p<0.05, \*\* <sup>b</sup> p<0.01 and \*\*\* <sup>c</sup> p<0.0001.

**Figure 3. Effect of metal ion combinations on osteoblast mineralization**

Mineralization was assessed in SaOS-2 cells cultured in osteogenic media for 7 days in the presence of metal ions. The graphs are depicted with metal ion concentrations compartmentalised corresponding to physiological, patient serum and patient hip aspirate levels post MOMHR. **A)** The effect of  $\text{Co}^{2+}:\text{Cr}^{3+}$  combinations at equal concentrations, and **B)** the effect of  $\text{Co}^{2+}:\text{Cr}^{6+}$  combinations at equal concentrations. All values (mean  $\pm$  95%CI)



are expressed relative to the vehicle (100%). n = 4-6 wells per experiment, 4 replicate experiments. \* <sup>a</sup> p<0.05, \*\* <sup>b</sup> p<0.01 and \*\*\* <sup>c</sup> p<0.0001.

#### **Figure 4. ALP activity of SaOS-2 cells on prosthesis surfaces**

ALP activity of SaOS-2 cells on prosthesis surfaces with metal ions and nanoparticles treatments was measured after 7 days. All values represented as mean ± 95%CI from 3 repeat experiments with 5 replicates per experiment. \* <sup>a</sup> p<0.05; <sup>b</sup> p<0.01; \*\*\* <sup>c</sup> p<0.0001.

#### **Figure 5. Effect of prosthesis surfaces on mineralization by osteoblasts**

**A)** Images of grit-blasted (GB), plasma-sprayed titanium coated (Ti) and plasma-sprayed hydroxyapatite coated (HA) surfaces used to assess osteoblast mineralization. **B)** Percentage mineralization on prosthesis surfaces measured using xylenol orange, a fluorochrome that incorporates into newly calcified matrix. **C)** Representative images of mineralization (grey) on prosthesis surfaces. <sup>a</sup> p<0.05 and <sup>c</sup> p<0.0001. Scale bar = 200µm.

#### **Figure 6. Effect of metal ions and nanoparticles on mineralization by SaOS-2 cells on prosthesis surfaces**

Mineralization by osteoblasts on prosthesis surfaces with metal ions and nanoparticle treatments represented as percentage response to the vehicle (y= 100). All values represented as mean ± 95%CI from 3 repeat experiments with 3 replicates per experiment. <sup>b</sup> p<0.01; <sup>c</sup> p<0.0001.

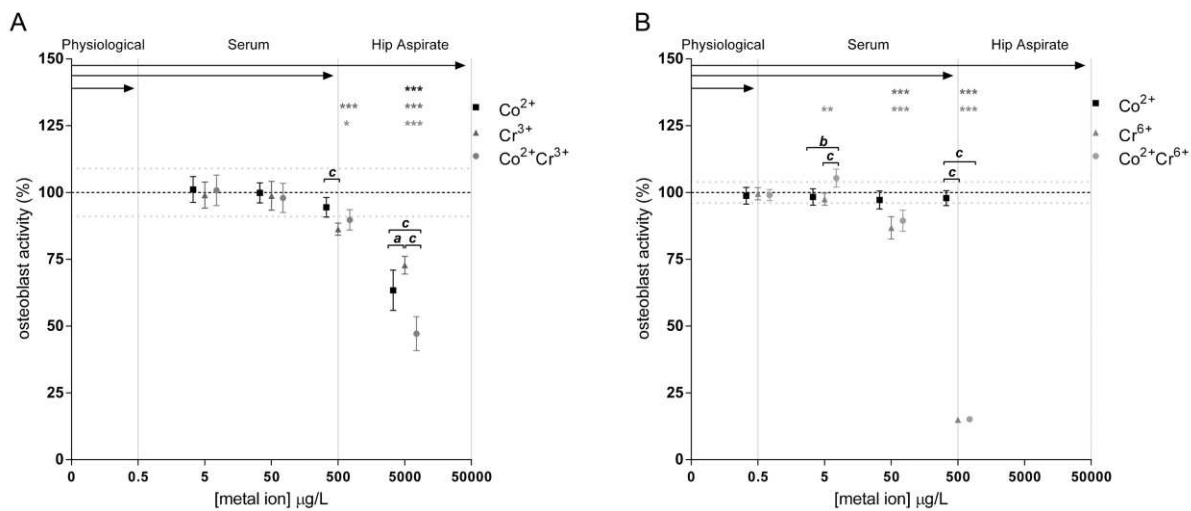


Figure 1

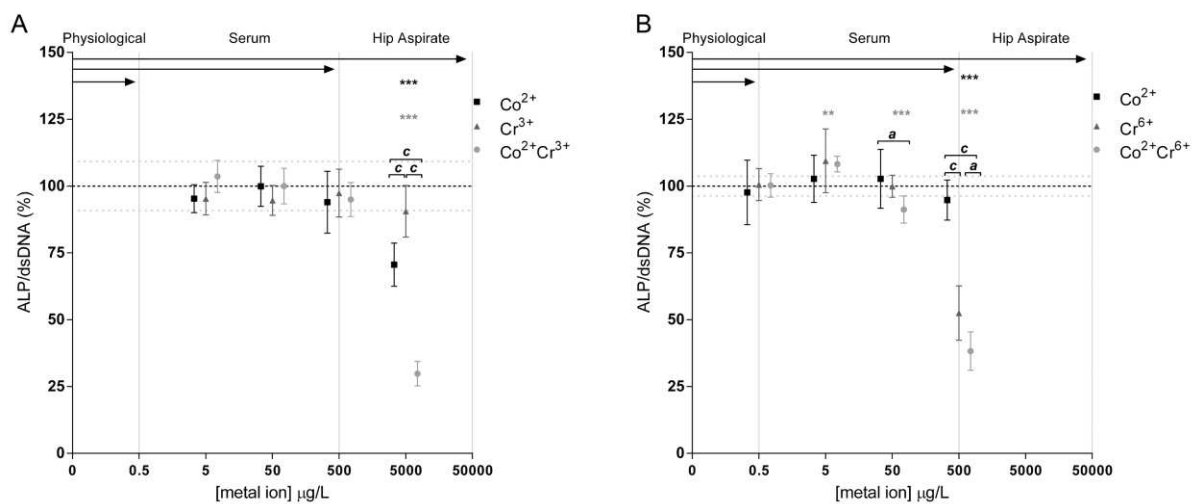


Figure 2

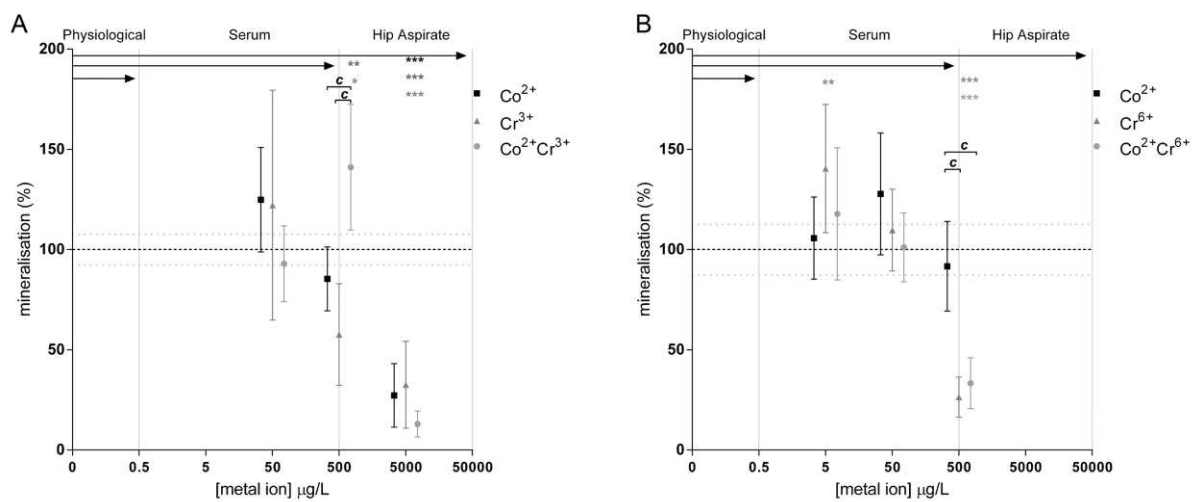


Figure 3

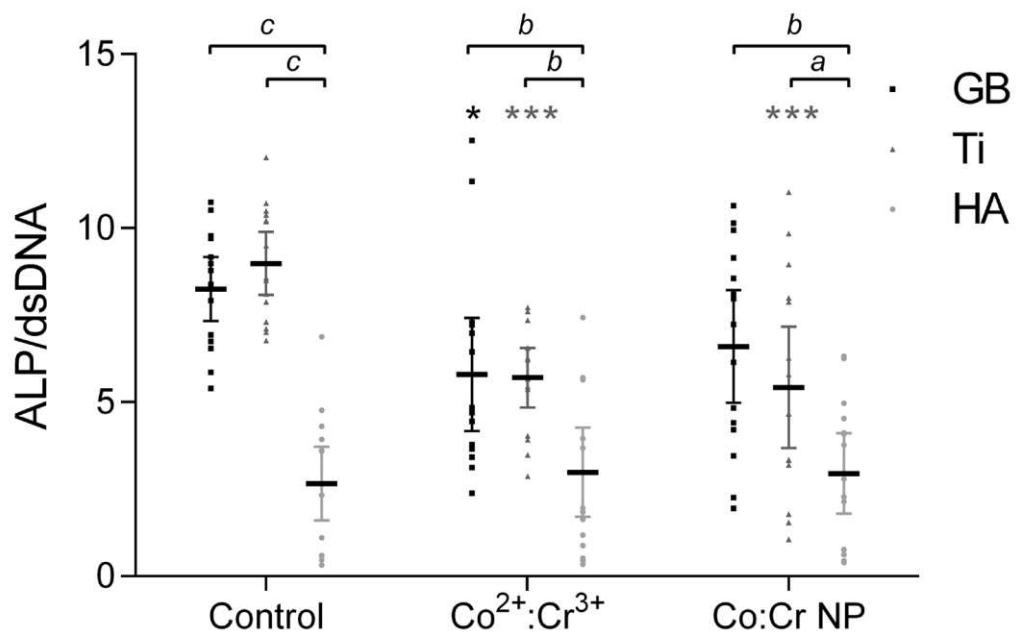


Figure 4



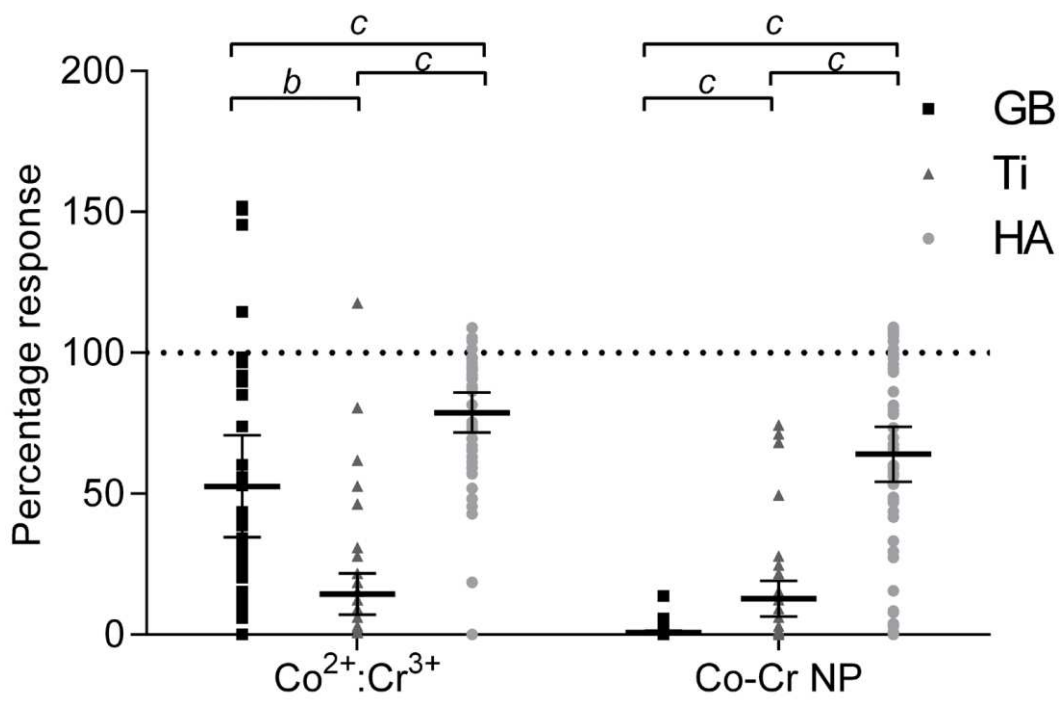


Figure 6